IEEE Access
Multidisciplinary | Rapid Review | Open Access Journal

Received February 13, 2019, accepted February 21, 2019, date of publication March 4, 2019, date of current version April 2, 2019.

Digital Object Identifier 10.1109/ACCESS.2019.2902596

High Gain Bow-Tie Slot Antenna Array Loaded With Grooves Based on Printed Ridge Gap Waveguide Technology

SYED M. SIFAT, (Graduate Student Member, IEEE), MOHAMED MAMDOUH M. ALI, (Student Member, IEEE), SHOUKRY I. SHAMS, (Member, IEEE), AND ABDEL-RAZIK SEBAK, (Life Fellow, IEEE)

Electrical and Computer Engineering Department, Concordia University, Montreal, QC H4B 1R6, Canada

Corresponding author: Syed M. Sifat (s_sifat@encs.concordia.ca)

ABSTRACT The development of wireless and satellite communication has led to a demand for high-performance microwaves and mm-wave components in terms of cost, losses, and fabrication complexity. Gap waveguide is one of the emerging technologies in 5G and mm-wave applications due to their low cost, low losses, and high power handling capability. In this paper, a groove-based wideband bow-tie slot antenna array is designed at 30 GHz based on printed ridge gap waveguide technology (PRGW). A two-section T-shaped ridge is designed to feed a bow tie slot placed on the upper ground of the PRGW. The gain of the proposed slot antenna is enhanced by using a horn-like groove. Then, the proposed high gain element is deployed to build up a 1 bow-tie slot antenna array loaded with three-layer groove antenna. The proposed antenna array is fabricated and measured, where the measured results show a −10-dB impedance bandwidth from 29.5 to 37 GHz (22%). The fabricated prototype achieves a high gain of 15.5 dBi and a radiation efficiency higher than 80% over the operating frequency bandwidth.

INDEX TERMS Millimeter wave technology, periodic structure, wideband, high gain, antenna arrays.

I. INTRODUCTION

Millimeter wave antennas for gigabit wireless communications endeavors to offer a comprehensive treatment of antennas based on wide bandwidth and high-speed data transmission. However, at high frequencies propagation losses are enormous compared to low-frequency bands. So high gain and wideband antennas are required to mitigate the losses in this frequency range [1], [2]. Microstrip lines work effectively at low frequencies with ultra wideband characteristics [3], [4]. On the other hand, at high frequencies, microstrip feeding networks suffer from high ohmic, dielectric losses and surface waves [5]–[7]. The rectangular or hollow waveguide has high Q-factor and low radiation losses at higher frequencies, however, the design complexity increases as the frequency increases [8], [9]. The sidewalls become very difficult to fabricate and ensuring the proper electrical contact becomes a big challenge. Substrate Integrated Waveguide (SIW) is another promising technology to design an efficient feeding network at millimeter wave frequency, where the electrical characteristics are similar to the traditional rectangular waveguide. SIW's have better radiation efficiency, while this efficiency degrades with large arrays [10], [11]. Therefore, an alternative guiding structure to the rectangular waveguide and microstrip lines at higher frequencies were introduced in 2009 namely ridge gap waveguide (RGW), which has low losses and high power handling capability [12].

Ridge gap waveguide (RGW) consists of two parallel plates, one plate with periodic textures to stop the wave propagation in all directions except the required path [13]. These periodic textured cells prevent the leakage and ensure a quasi TEM mode inside this air gap. In other words, using periodic cells, artificial magnetic conductor (AMC) surface can be created, which can create a parallel-plate bandgap [14]. In the past decade, RGW was utilized in many applications to design microwave components and devices [15]–[17].

The associate editor coordinating the review of this manuscript and approving it for publication was Mengmeng Li.

Moreover, this guiding structure was deployed to implement various types of antennas and antenna feeding networks. However, many of the published antenna structures were limited in terms of the operating bandwidth, especially RGW fed slot antennas [18], [19]. Some possible techniques were implemented to enhance the antenna bandwidth, like adding a T-junction at the end of the ridge [20]. Besides, slot antenna arrays with cavity layers were used for a high gain purpose [21]. On the other hand, using cavities makes the overall antenna very bulky and it is not appropriate for all the applications. The RGW has shown promising results; however, the need for high accuracy CNC machining is a major drawback for this configuration. As a result, many articles were published to propose a printed version of RGW for better integrability and lower cost.

Recently, the Printed Ridge Gap Waveguide (PRGW) has drawn a lot of attention due to its low losses at mm-wave bands [22]–[27]. Although PRGW is built on a PCB, it will not be accountable for dielectric losses, as the wave is propagating inside an air gap. Various directive antennas and arrays based on PRGW have already been proposed with improved impedance bandwidth and high gain. The magneto electro dipole and superstrate were used to improve the bandwidth, gain and cross polarizations [28]–[30]. Even the gain is improved significantly using superstrates, however, the bandwidth does not exhibit more than 20% impedance bandwidth and the antenna array suffers from grating lobes [26], [30]. Moreover, DRA was added on top of the coupling slot of PRGW to enhance the impedance bandwidth, which can extend the bandwidth to 20% [31]. To solve the bandwidth and grating lobe issues, simultaneously, this paper provides a solution featured with bandwidth, low side lobe level and high gain as well as it provides a strong mechanical support to the overall antenna structure and stable radiation pattern over the frequency range.

In this work, a two-section T-shaped ridge with a bow-tie slot is used to enhance the matching level and impedance bandwidth of the antenna. Later a step rectangular horn is placed upon the bow tie slot for gain enhancement. The metallic groove layers give additional mechanical support to hold the structure. Moreover, we have designed 1×4 antenna array using PRGW and afterward, it is loaded with three layers of a groove to enhance the gain with sidelobe level below -13 dB for both E- and H-plane. Microstrip-PRGW transitions were used to feed the transmission line, and the matching bandwidth is more than 22%. The antenna design is illustrated in section III, while the 1×4 feeding network illustrated in section IV. Section V shows the configuration of 1×4 integrated antenna array and section VI represents the measurement results for the fabricated prototype.

II. UNIT CELL ANALYSIS AND DESIGN OF WAVEGUIDE

The main characteristics of a gap waveguide are its ability to create parallel plate stopband using the periodic structures [12]. The proposed unit cell with ridge is illustrated in Fig. 1(a), where the dispersion diagram for this section of

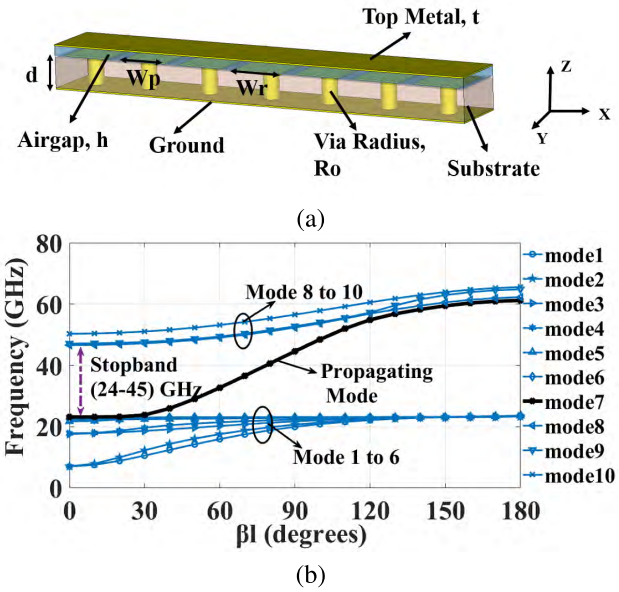

FIGURE 1. (a) Structure of one row of unit cells with ridge. (b) Dispersion diagram with the ridge existence.

TABLE 1. Dimensions of unit cell with ridge.

Parameters	Value in (mm)
Substrate thickness, d	0.75
Patch Width, Wp	1.2
Ridge Width, Wr	1.3
Radius of Via, Ro	0.1875
Airgap, h	0.254

PRGW line is shown in Fig. 1(b). The dispersion diagram is calculated using Eigen Mode Solver (CST Microwave Studio), which exhibits the realized bandgap of the periodic structure. The unit cell is printed on Rogers RO3003 with a ϵ_r of 3, and all the other required dimensions are illustrated in Table 1.

The realized bandgap of one row of the unit cell with ridge is over 24-45 GHz, which can be depicted from the dispersion diagram in Fig. 1(b). The proposed waveguide is a multilayer structure and to feed the PRGW; a microstrip-PRGW transition is used as illustrated in Fig. 2(a). The proposed 3-D view shows how the transition is aligned, and the proper placing of the feedline is demonstrated. The microstrip to ridge transition has been investigated in details in many published articles [22]–[24]. The S-parameter of the microstrip-PRGW transition is illustrated in Fig. 2(b) and it is clear that the transmission coefficient is close to -0.5 ± 0.2 dB, which is due to the insertion losses from the microstrip transitions input/output lines in the whole operational bandwidth.

III. ANTENNA DESIGN

In our work, a two-section T-shaped ridge with a bow-tie slot is used to provide a wide bandwidth. Slot antenna itself has a narrow bandwidth of around 4-5 % at the center frequency. The proposed single element antenna is shown in Fig. 3 with proper dimensions listed in Table 2.

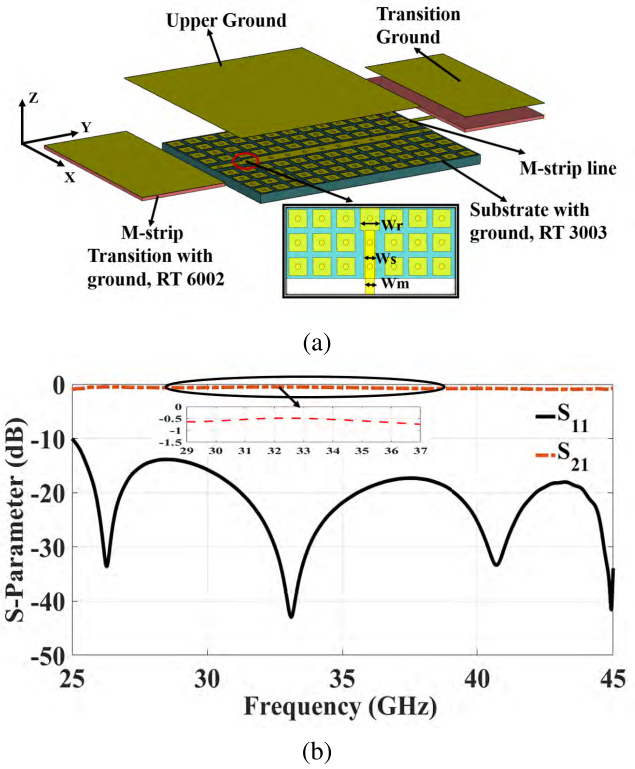

FIGURE 2. (a) Proposed microstrip-ridge transition. (b) Simulated S-parameter of the printed ridge gap waveguide transition.

The single element PRGW antenna consists of three layers; the first one is the ridge with periodic cells; the second layer is the bow-tie antenna that is printed on the Rogers RO6002 substrate. Finally, a three-layer groove structure on top of the bow-tie slot is deployed, where all layers have a total thickness of 4.5 mm. We have preferred step-shaped aperture for our design as it's a cost-effective technique that can be realized using our fabrication facilities. Here the groove dimensions were only increased in one axis, as shown in Fig. 3(d). The simulated reflection coefficient and the gain for the single element antenna with and without the horn-like groove structure is illustrated in Fig. 4(a) and 4(b), respectively. It can be observed that using groove layers enhanced the antenna bandwidth up to 20.6% from (29-35.6) and the gain is increased by 3 dB over the whole frequency range over 29-37 GHz after adding the groove layer. Besides, the E- and H-plane radiation patterns for the proposed antenna with and without the horn-like groove structure are shown in Fig. 4(c) at the center operating frequency. From this figure, it can be depicted that due to the groove layer the beam in the E-plane became narrower and a high gain is obtained.

In our work, for the three-layer groove section, the dimensions in the H-plane are kept constant, and in the E-plane, the dimensions are varied in stepped size, which resulted in an overall increase in the aperture area that provides a higher gain. Some parametric studies were done to choose the optimum value for this design which is illustrated in Fig. 5.

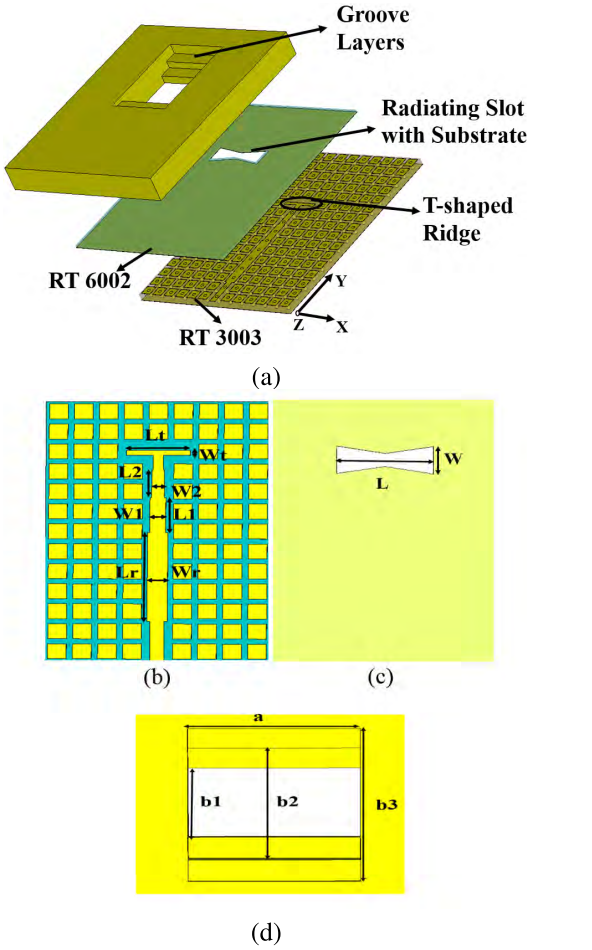

FIGURE 3. (a) Proposed 3D model for the single element bow-tie groove. (b) Feeding layer. (c) Bow-tie slot antenna layer. (d) Horn-like groove layer.

TABLE 2. Dimensions of single element PRGW antenna (in mm).

Dimension	Value	Dimension	Value
Slot length, L	6.4	Slot width, W	2.7
Ridge length, Lr	7.8	Ridge width, Wr	1.3
M-Strip Width, Wm	0.62	Strip width, Ws	0.75
1st Section, L1	2.8	1st Section, W1	1.015
2nd Section, L2	2.2	1st Section, W2	0.81
3rd Section, L3	1.2	3rd Section, W3	0.63
T-Section, Lt	4.1	T-Section, Wt	0.4
Groove width, a	7.5	Layer 1 width, b1	5
Layer 2 width, b2	8	Layer 3 width, b3	11

IV. 1 × 4 BOW-TIE SLOT ANTENNA ARRAY USING PRGW

In this section, the design of a 1× 4 Bow-tie slot antenna array using the PRGW technology is proposed. Initially, a 1 × 2 feeding network is designed with a matching level <−15 dB over 29-37 GHz. Then, a 1 × 4 power divider is constructed using the two-way feeding network, where the schematic view is shown in Fig. 6(a) with all the required designed parameters. The S-parameter of the 1 × 4 power divider is shown in Fig. 6(b), where the matching bandwidth level is below −15 dB in the required frequency band. The transmission coefficient to each port is around −6.5 dB over 29-37 GHz. This power divider is deployed to feed four

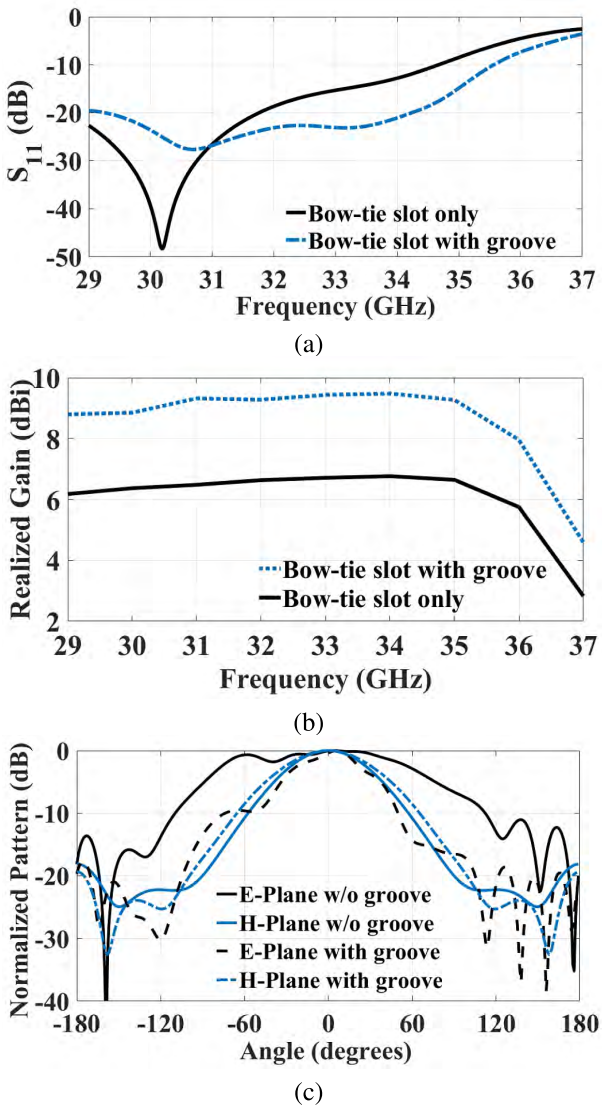

FIGURE 4. (a) Simulated reflection coefficient of single element PRGW antenna. (b) Gain versus the frequency comparison for the single element. (c) Simulated radiation pattern comparison for single element at 30 GHz.

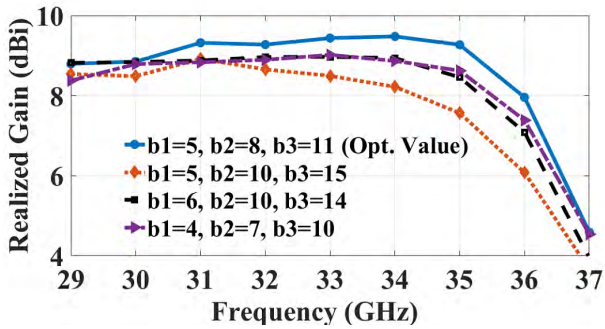

FIGURE 5. Simulated gain comparison by changing groove size.

Bow-tie slot antenna elements as illustrated in Fig. 7(a), where the reflection coefficient of the proposed array is shown in Fig. 7(b). It can be depicted that the proposed array structure gives an extended bandwidth of 22.7%. The element to element spacing of the slot antenna is kept 0.8 λ_o to avoid

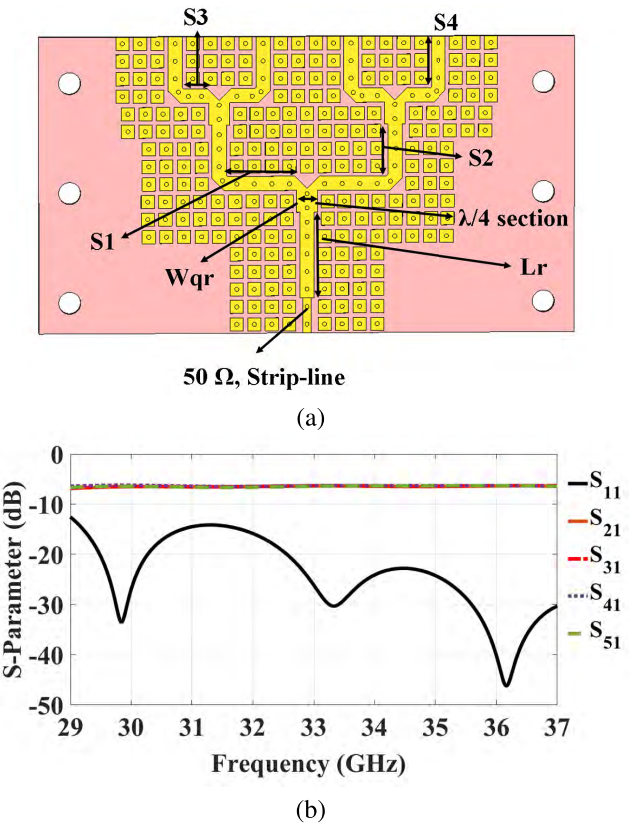

FIGURE 6. (a) Simulated layout of 1 × 4 power divider. (b) Simulated S-parameter of the power divider.

TABLE 3. Dimensions of PRGW antenna array (in mm).

Dimension	Value	Dimension	Value
Lqr	2.4	Wqr	1.9
S1	8.65	S2	4.9
S3	4.65	S4	5.8
Lg	32	Wg	14

the grating lobes, where λ_o is the free-space wavelength at 30 GHz. The design parameters of the 1 × 4 power divider are described in Table 3. The radiation patterns of the 1 × 4 Bow-tie slot antenna array are shown in Fig. 8 for the E- and H-plane at 30, 32 and 34 GHz. It shows clearly that the sidelobe level (SLL) is less than −13 dB with a stable gain as shown in Fig. 7(b) throughout the frequency range over 29-37 GHz. The proposed antenna array has a narrow beam in the H-plane due to the four-element array and a wide beam in the E-plane mainly due to the element pattern.

V. THREE LAYER GROOVE ARRAY WITH 1 × 4 BOW-TIE ANTENNA ARRAY

In this work, we have proposed a three-layer groove antenna array loaded on top of the designed bow-tie slot antenna array. Our main objective of this work is to propose an antenna with high gain and wide bandwidth so that it can fulfill the requirement of mm-wave communication. The proposed 1 × 4 groove antenna array is shown in Fig. 9(a). The reflection coefficient of the linear array antenna is illustrated in Fig. 9(b), which covers a 22% bandwidth

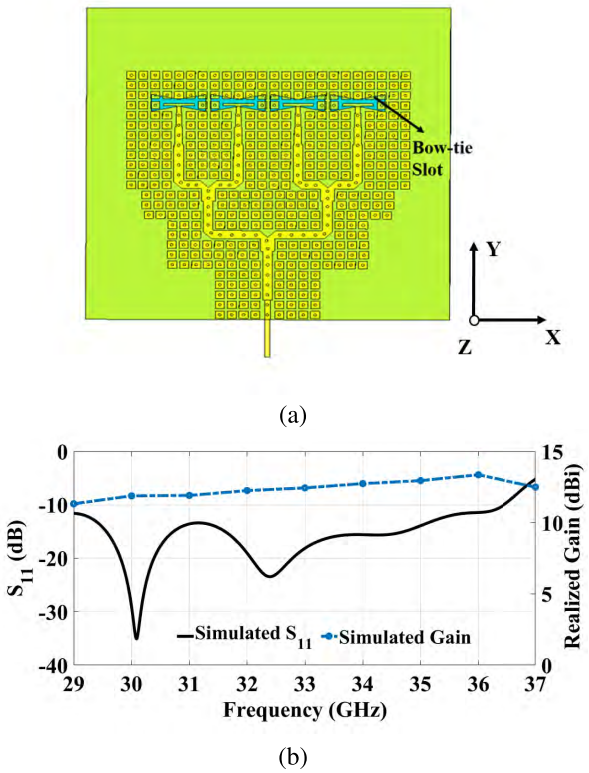

FIGURE 7. (a) The simulated model top view of the bow-tie slot antenna array. (b) Reflection coefficient and gain of 1 × 4 bow-tie antenna array.

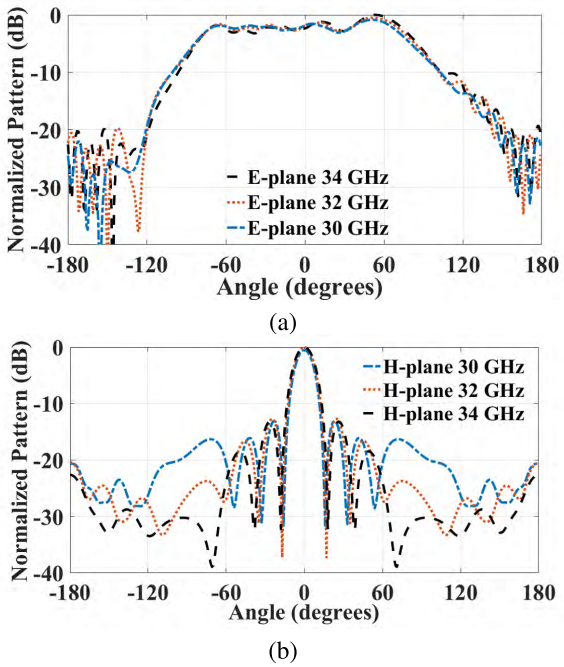

FIGURE 8. Simulated normalized radiation pattern of the bow-tie antenna array. (a) E-plane. (b) H-plane.

of 29.4-36.8 GHz. Besides, the proposed array achieves a gain of 14.5 ± 1 dBi over the whole frequency band.

The radiation patterns of the linear array antenna for E- and H-plane are illustrated for various frequencies

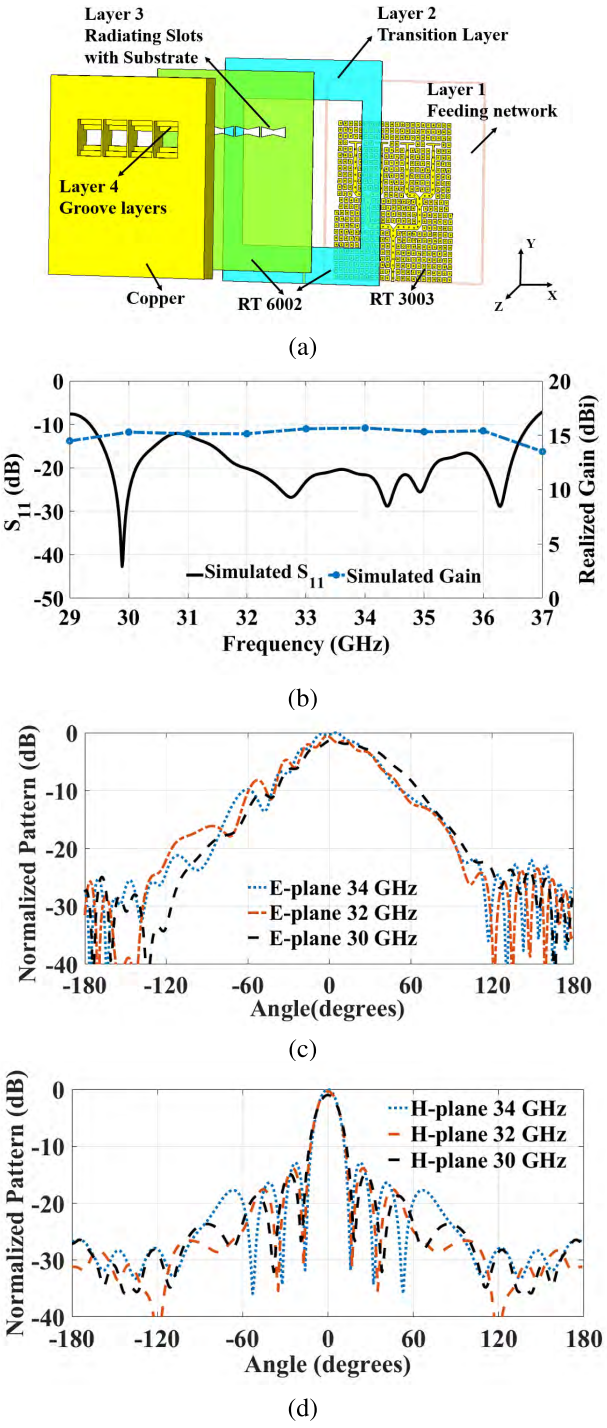

FIGURE 9. (a) 3D view of the proposed 1 × 4, three layer groove antenna array. (b) Simulated reflection coefficient and gain of 1 × 4 groove antenna array. (c) Simulated E-plane radiation pattern of groove antenna array. (d) Simulated H-plane radiation pattern of groove antenna array.

in Fig. 9(c) and 9(d) respectively. As shown in Fig. 9(a) the antenna elements are placed linearly in the x-direction which results in narrower beam width in the H-plane, while a wide beam width is achieved in the E-plane. As a result, the radiation pattern is affected in the E-plane as the groove edges in the y-direction are close to the antenna element, which results in a slight stable radiation pattern in the E-plane. To avoid the

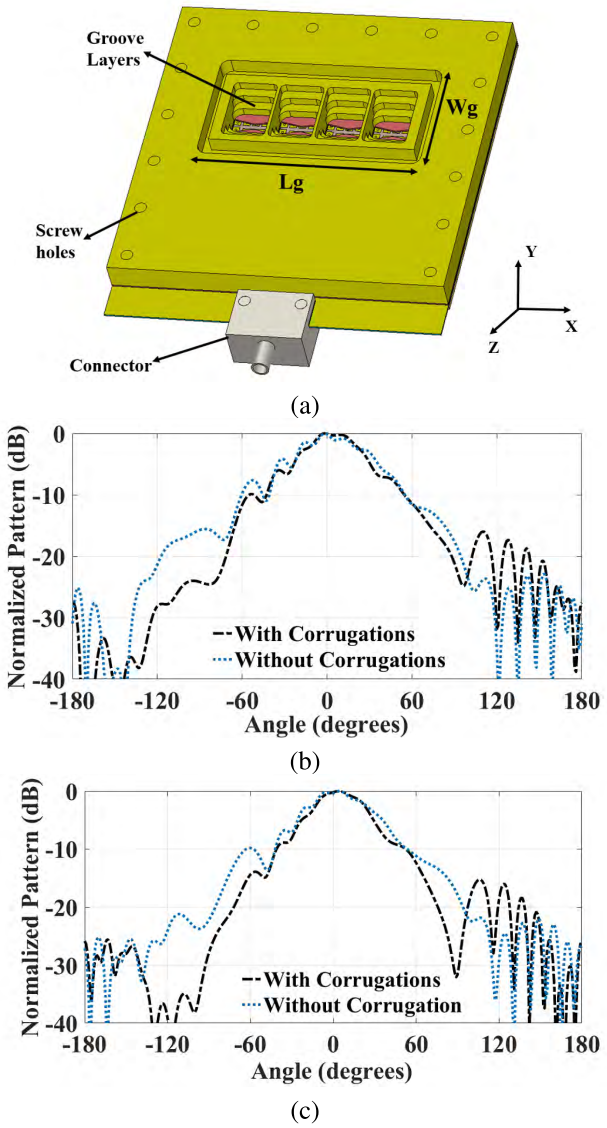

FIGURE 10. (a) Improved 3-D, 1 × 4 groove antenna array with corrugations. (b) Simulated E-plane radiation pattern comparison at 32 GHz. (c) Simulated E-plane radiation pattern comparison at 34 GHz.

increase in the antenna size a corrugation layer is added to improve the E-plane radiation pattern. This corrugation layer acts as an artificial magnetic ring surrounding the antenna array, which decreases the surface wave and accordingly enhances the radiation pattern. The improved linear antenna array structure is illustrated in Fig. 10(a) with a corrugation layer and the improvement in the E-plane radiation patterns are shown in Fig. 10(b) and 10(c), at 32 and 34 GHz, respectively. By adding the single corrugation layer, the E-plane radiation pattern improved significantly without increasing the antenna dimensions. This corrugation technique is generally applied to reduce sidelobe levels and to reduce cross polarizations.

VI. EXPERIMENTAL AND VALIDATION

To validate the proposed design an array of 1 × 4 integrated antenna is fabricated and measured where the photos of the

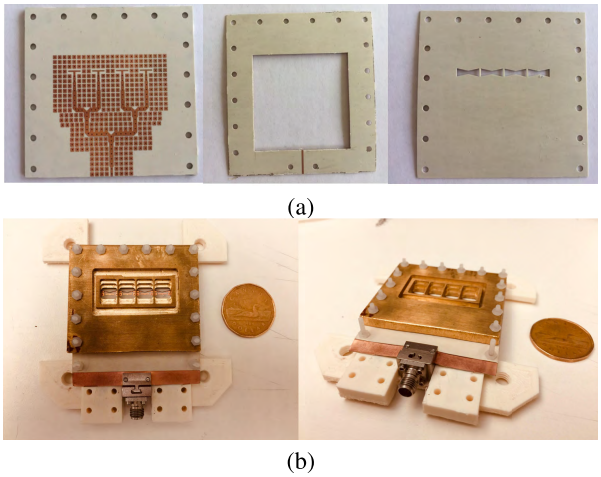

FIGURE 11. (a) Prototype layers. (b) Final assembly of 1 × 4 integrated antenna array.

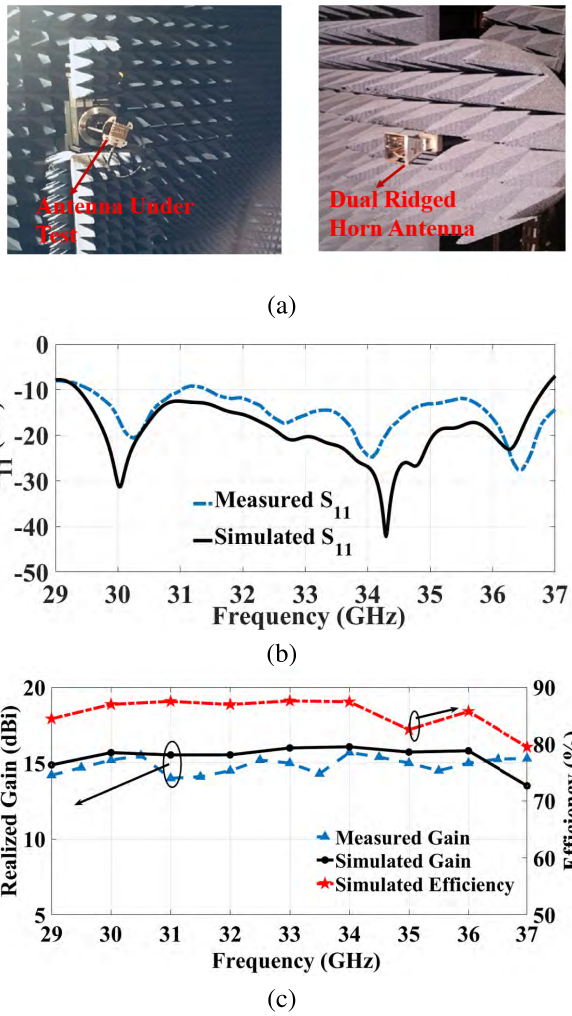

FIGURE 12. (a) Radiation pattern measurement setup in the anechoic chamber. (b) Measured reflection coefficient of the fabricated antenna array. (c) Measured gain of the fabricated antenna array.

fabricated parts are illustrated in Fig. 11(a). The fabricated layers are assembled using plastic screws, where the assembled prototype is shown in Fig. 11(b). The $|S_{11}|$ is measured using an N52271A phase network analyzer, where the

TABLE 4. Comparison of proposed antenna array with some previously published work.

Ref	Frequency (GHz)	Antenna Type	Size	Bandwidth (%)	Gain(dBi)	Rad. efficiency
This work	30	1 x 4 Slot antenna	$4\lambda_o$ x 4.2 λ_o x 0.53 λ_o	22	15.5	87% (simulated)
[28]	95	1 x 8 ME dipole	$8.25\lambda_o$ x 5.4 λ_o x 3.6 λ_o	14.5	16.5	Not mentioned
[29]	30	4 x 4 ME dipole	$3.5\lambda_o$ x 3.4 λ_o x 0.28 λ_o	16.5	21.2	70% (measured)
[26]	60	SIW Cavity	Not mentioned	16	21	Not mentioned
[27]	30	2 x 2 ME dipole	5.6 λ_o x 7.1 λ_o x 0.28 λ_o	20	10.3	84% (simulated)

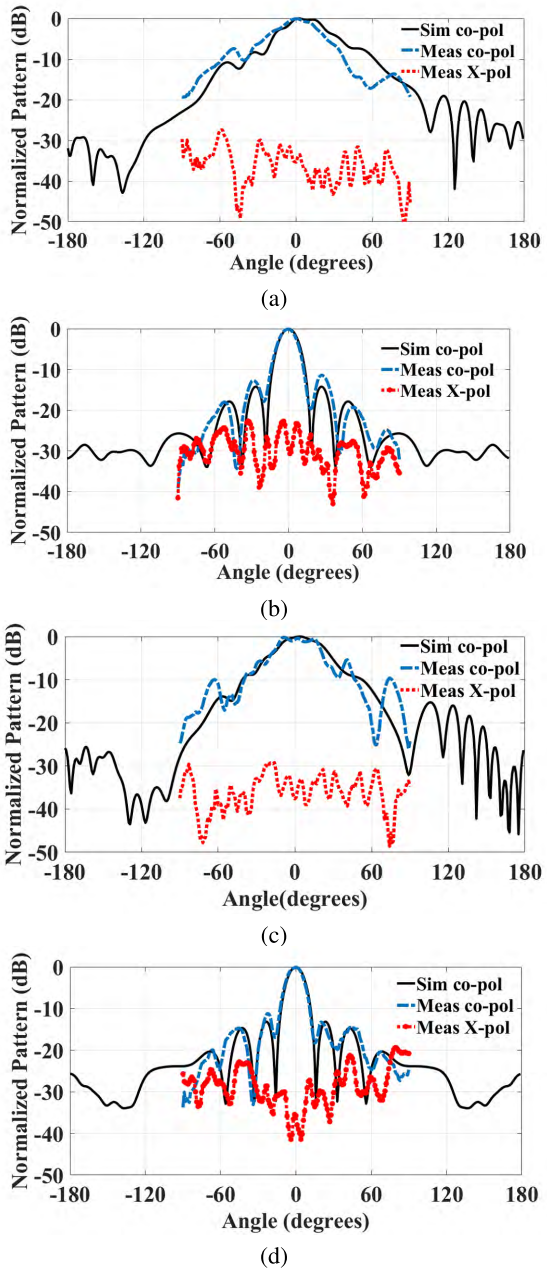

FIGURE 13. Comparison of measured and simulated normalized radiation pattern. (a) E-plane 30 GHz, (b) H-plane 30 GHz, (c) E-plane 34 GHz, and (d) H-plane 34 GHz.

measured and simulated reflection coefficient are illustrated in Fig. 12(b). It can be noticed that a 22 % impedance bandwidth with $|S_{11}| < -10$ dB is achieved from the proposed prototype, where there is a slight shift in the frequency response occurred with a bit above -10 dB over 31-31.5 GHz. The gain and radiation pattern are measured in the anechoic chamber system, as shown in Fig. 12(a).

It is worth mentioning that, in our measurement set up, we don't have the facility to calculate measured radiation efficiency. The measured and simulated gain of the proposed array is shown in Fig. 12(c). This figure shows that the measured gain is 15 $\pm$ 1 dBi. The fabrication tolerance for antenna layers as well as the groove may affect the measured results. The measured radiation pattern in E- and H-plane is illustrated in Fig. 13. The measured co polarizations of the antenna in both E- and H-plane are in a good agreement, and the cross polarizations are low in both E- and H-plane.

Table 4 shows a comparison between the proposed work and previous works. The proposed antenna exhibits superior characteristics at mm-wave frequency bands including low loss, self-packaged and planar structure. In [26], the SIW cavity antenna array suffers from the grating lobes where the SLL is less than -6.5 dB at high frequencies, which restricts its application. In addition, for 2D beam scanning purpose, ME dipole array was fed by the RGW Butler matrix to provide stable radiation pattern and wide bandwidth [27]. However, the gain and radiation efficiency of the antenna is low compared to our work. An array of 1×8 aperture coupled ME dipole was proposed in [28], for circular polarization applications, however, the ME dipole antenna provides only 14.5 % bandwidth and the size of the antenna are very large compared to our proposed antenna. In [29], 4×4 ME dipole antenna was used for high gain and wideband purpose, however, the bandwidth is less than our proposed work. Our proposed antenna provides wideband, high gain, better efficiency as well as strong mechanical support compared to the other published designs.

VII. CONCLUSION

In this work, we have presented a high gain, a wideband antenna array, based on the PRGW technology. It has lower losses compared to printed microstrip lines. A bow-tie slot antenna is utilized to get a wide impedance bandwidth, while a three-layer groove structure is deployed to provide strong mechanical support and enhance the gain. The fabricated prototype achieves a high gain of 15.5 dBi over the operating frequency bandwidth. The fabricated prototype gives 22% impedance bandwidth where a good agreement between both the measured and the simulated response has been shown.

REFERENCES

[1] K.-C. Huang and D. J. Edwards, *Millimetre Wave Antennas for Gigabit Wireless Communications*. New York, NY, USA: Wiley, 2008.

[2] Y. Wang, J. Li, L. Huang, Y. Jing, A. Georgakopoulos, and P. Demestichas, "5G mobile: Spectrum broadening to higher-frequency bands to support high data rates," *IEEE Veh. Technol. Mag.*, vol. 9, no. 3, pp. 39–46, Sep. 2014.
[3] M. M. Azer, S. I. Shams, and A. M. M. A. Allam, "Compact double-sided printed omni-directional ultra wideband antenna," in *Proc. 14th Int. Symp. Antenna Technol. Appl. Electromagn. (ANTEM)*, Ottawa, ON, Canada, Jul. 2010, pp. 1–4.
[4] S. M. Sifat, S. I. Shams, and A. R. Sebak, "High gain wideband log periodic dipole array antenna loaded with corrugations," in *Proc. 18th Int. Symp. Antenna Technol. Appl. Electromagn. (ANTEM)*, Waterloo, ON, Canada, Aug. 2018, pp. 1–2.
[5] A. Borji, D. Busuioc, and S. Safavi-Naeini, "Efficient, low-cost integrated waveguide-fed planar antenna array for Ku-band applications," *IEEE Antennas Wireless Propag. Lett.*, vol. 8, pp. 336–339, 2009.
[6] D. M. Pozar, "Considerations for millimeter wave printed antennas," *IEEE Trans. Antennas Propag.*, vol. AP-31, no. 5, pp. 740–747, Sep. 1983.
[7] E. Levine, G. Malamud, S. Shtrikman, and D. Treves, "A study of microstrip array antennas with the feed network," *IEEE Trans. Antennas Propag.*, vol. 37, no. 4, pp. 426–434, Apr. 1989.
[8] M. M. M. Ali, S. I. Shams, and A.-R. Sebak, "Low loss and ultra flat rectangular waveguide harmonic coupler," *IEEE Access*, vol. 6, pp. 38736–38744, 2018.
[9] M. M. M. Ali, S. I. Shams, A. Sebak, and A. A. Kishk, "Rectangular waveguide cross-guide couplers: Accurate model for full-band operation," *IEEE Microw. Wireless Compon. Lett.*, vol. 28, no. 7, pp. 561–563, Jul. 2018.
[10] W. Han, F. Yang, J. Ouyang, and P. Yang, "Low-cost wideband and high-gain slotted cavity antenna using high-order modes for millimeter-wave application," *IEEE Trans. Antennas Propag.*, vol. 63, no. 11, pp. 4624–4631, Nov. 2015.
[11] J. Wu, Y. J. Cheng, and Y. Fan, "60-GHz substrate integrated waveguide fed cavity-backed aperture-coupled microstrip patch antenna arrays," *IEEE Trans. Antennas Propag.*, vol. 63, no. 3, pp. 1075–1085, Mar. 2015.
[12] P.-S. Kildal, E. Alfonso, A. Valero-Nogueira, and E. Rajo-Iglesias, "Local metamaterial-based waveguides in gaps between parallel metal plates," *IEEE Antennas Wireless Propag. Lett.*, vol. 8, no. 4, pp. 84–87, Apr. 2009.
[13] P.-S. Kildal, A. U. Zaman, E. Rajo-Iglesias, E. Alfonso, and A. Valero-Nogueira, "Design and experimental verification of ridge gap waveguide in bed of nails for parallel-plate mode suppression," *IET Microw., Antennas Propag.*, vol. 5, no. 3, pp. 262–270, Mar. 2011.
[14] D. Sievenpiper, L. Zhang, R. F. J. Broas, N. G. Alexopolous, and E. Yablonovitch, "High-impedance electromagnetic surfaces with a forbidden frequency band," *IEEE Trans. Microw. Theory Techn.*, vol. 47, no. 11, pp. 2059–2074, Nov. 1999.
[15] M. S. Sorkherizi, A. Khaleghi, and P.-S. Kildal, "Direct-coupled cavity filter in ridge gap waveguide," *IEEE Trans. Compon., Packag., Manuf. Technol.*, vol. 4, no. 3, pp. 490–495, Mar. 2014.
[16] S. I. Shams and A. A. Kishk, "Wide band power divider based on Ridge gap waveguide," in *Proc. 17th Int. Symp. Antenna Technol. Appl. Electromagn. (ANTEM)*, Montreal, QC, Canada, Jul. 2016, pp. 1–2.
[17] S. I. Shams and A. A. Kishk, "Design of 3-dB hybrid coupler based on RGW technology," *IEEE Trans. Microw. Theory Techn.*, vol. 65, no. 10, pp. 3849–3855, Oct. 2017.
[18] A. Sahu, V. Devabhaktuni, and P. H. Aaen, "A slot anntenna designed in ridge gap waveguide technology for V-band applications," in *Proc. IEEE MTT-S Int. Microw. RF Conf. (IMaRC)*, Hyderabad, India, Dec. 2015, pp. 385–387.
[19] A. U. Zaman and P. Kildal, "A new 2×2 microstrip patch sub-array for 60 GHz wideband planar antenna with ridge gap waveguide distribution layer," in *Proc. 9th Eur. Conf. Antennas Propag. (EuCAP)*, Lisbon, Portugal, 2015, pp. 1–4.
[20] A. U. Zaman and P.-S. Kildal, "Wide-band slot antenna arrays with single-layer corporate-feed network in ridge gap waveguide technology," *IEEE Trans. Antennas Propag.*, vol. 62, no. 6, pp. 2992–3001, Jun. 2014.
[21] D. Zarifi, A. Farahbakhsh, A. U. Zaman, and P. S. Kildal, "Design and fabrication of a high-gain 60-GHz corrugated slot antenna array with ridge gap waveguide distribution layer," *IEEE Trans. Antennas Propag.*, vol. 64, no. 7, pp. 2905–2913, Jul. 2016.
[22] H. Raza, J. Yang, P.-S. Kildal, and E. A. Alós, "Microstrip-ridge gap waveguide–study of losses, bends, and transition to WR-15," *IEEE Trans. Microw. Theory Techn.*, vol. 62, no. 9, pp. 1943–1952, Sep. 2014.
[23] E. Pucci, E. Rajo-Iglesias, and P.-S. Kildal, "New microstrip gap waveguide on mushroom-type EBG for packaging of microwave components," *IEEE Microw. Wireless Compon. Lett.*, vol. 22, no. 3, pp. 129–131, Mar. 2012.
[24] M. S. Sorkherizi and A. A. Kishk, "Fully printed gap waveguide with facilitated design properties," *IEEE Microw. Wireless Compon. Lett.*, vol. 26, no. 9, pp. 657–659, Sep. 2016.
[25] M. M. M. Ali, S. I. Shams, and A. R. Sebak, "Printed ridge gap waveguide 3-dB coupler: Analysis and design procedure," *IEEE Access*, vol. 6, pp. 8501–8509, 2018.
[26] S. A. Razavi, P.-S. Kildal, L. Xiang, E. A. Alós, and H. Chen, "2 × 2-slot element for 60-GHz planar array antenna realized on two doubled-sided PCBs using SIW cavity and EBG-type soft surface fed by microstrip-ridge gap waveguide," *IEEE Trans. Antennas Propag.*, vol. 62, no. 9, pp. 4564–4573, Sep. 2014.
[27] M. M. M. Ali and A. Sebak, "2-D scanning magneto-electric dipole antenna array fed by RGW Butler matrix," *IEEE Trans. Antennas Propag.*, Nov. 2018.
[28] J. Cao, H. Wang, S. Mou, S. Quan, and Z. Ye, "W-band high-gain circularly polarized aperture-coupled magneto-electric dipole antenna array with gap waveguide feed network," *IEEE Antennas Wireless Propag. Lett.*, vol. 16, pp. 2155–2158, 2017.
[29] M. S. Sorkherizi, A. Dadgarpour, and A. A. Kishk, "Planar high-efficiency antenna array using new printed ridge gap waveguide technology," *IEEE Trans. Antennas Propag.*, vol. 65, no. 7, pp. 3772–3776, Jul. 2017.
[30] H. Attia, M. S. Sorkherizi and A. A. Kishk, "60 GHz slot antenna array based on ridge gap waveguide technology enhanced with dielectric superstrate," in *Proc. 9th Eur. Conf. Antennas Propag. (EuCAP)*, Lisbon, Portugal, 2015, pp. 1–4.
[31] H. Attia and A. A. Kishk, "Wideband self-sustained DRA fed by printed ridge gap waveguide at 60 GHz," in *Proc. IEEE 28th Annu. Int. Symp. Pers., Indoor, Mobile Radio Commun. (PIMRC)*, Montreal, QC, Canada, Oct. 2017, pp. 1–3.

SYED M. SIFAT (GS'18) received the B.Sc. degree in electrical and electronic engineering from American International University, Bangladesh, Dhaka, in 2013. He is currently pursuing the M.Sc. degree in electrical and computer engineering with Concordia University, Montreal, QC, Canada. Since 2017, he has been a Research Assistant with Concordia University. Before he joined the master's degree, he was with the City Group of Industries and GSL Export Ltd., in Bangladesh, as a Project Engineer. His research interests include designing mm-wave antennas, microwave circuits, gap waveguides, and periodic structures.

MOHAMED MAMDOUH M. ALI (S'15) received the B.Sc. (Hons.) and M.Sc. degrees in electronics and communications engineering from Assiut University, Egypt, in 2010 and 2013, respectively. He is currently pursuing the Ph.D. degree in electrical and computer engineering from Concordia University, Montreal, QC, Canada, in 2016. From 2010 to 2015, he was a Teaching and Research Assistant with the Department of Electronics and Communications Engineering, Assiut University. He was a Teaching and Research Assistant with Concordia University. His current research interests include microwave reciprocal/nonreciprocal design and analysis, and antenna design.

SHOUKRY I. SHAMS (M'04) received the B.Sc. (Hons.) and M.Sc. degrees in electronics and communications engineering from Cairo University, Egypt, in 2004 and 2009, respectively, and the Ph.D. degree in electrical and computer engineering from Concordia University, Montreal, QC, Canada, in 2016. From 2005 to 2006, he was a Teaching and Research Assistant with the Department of Electronics and Communications Engineering, Cairo University. From 2006 to 2012, he was a Teaching and Research Assistant with the IET Department, German University in Cairo. From 2012 to 2016, he was a Teaching and Research Assistant with Concordia University. His research interests include microwave reciprocal/nonreciprocal design and analysis, high power microwave subsystems, antenna design, and material measurement. He has received the Faculty Certificate of Honor, in 1999. He was a recipient of the Concordia University Recruitment Award, in 2012, and the Concordia University Accelerator Award, in 2016. He was the GUC-IEEE Student Branch Chair, from 2010 to 2012.

ABDEL-RAZIK SEBAK (LF'18) received the B.Sc. degree (Hons.) in electrical engineering from Cairo University, Cairo, Egypt, in 1976, the B.Sc. degree in applied mathematics from Ein Shams University, Cairo, in 1978, and the M.Eng. and Ph.D. degrees in electrical engineering from the University of Manitoba, Winnipeg, MB, Canada, in 1982 and 1984, respectively. From 1984 to 1986, he was with Canadian Marconi Company, where he was involved in the design of microstrip phased array antennas. From 1987 to 2002, he was a Professor with the Department of Electronics and Communication Engineering, University of Manitoba. He is currently a Professor with the Department of Electrical and Computer Engineering, Concordia University, Montreal, QC, Canada. His research interests include phased array antennas, millimeter-wave antennas and imaging, computational electromagnetics, and the interaction of EM waves with engineered materials and bioelectromagnetics. He is a member of the Canadian National Committee of the International Union of Radio Science Commission B. He was a recipient of the 1992 and 2000 University of Manitoba Merit Award for outstanding teaching and research, the 1994 Rh Award for outstanding contributions to scholarship and research, and the 1996 Faculty of Engineering Superior. He has served as the Chair of the IEEE Canada Awards and Recognition Committee, from 2002 to 2004, and as the Technical Program Chair of the 2002 IEEE CCECE Conference, and the 2006 URSIANTEM Symposium. He is the Technical Program Co-Chair of the 2015 IEEE ICUWB Conference.